PHOTONIC SENSORS / Vol. 9, No. 4, 2019: 293–301

• Fiber sensors, fiber devices, and related topics •

Trace Ammonia Detection Based on Near-Infrared Fiber-Optic Cantilever-Enhanced Photoacoustic Spectroscopy

Min GUO, Ke CHEN*, Zhenfeng GONG, and Qingxu YU

School of Optoelectronic Engineering and Instrumentation Science, Dalian University of Technology, Dalian 116024, China

*Corresponding author: Ke CHEN E-mail: chenke@dlut.edu.cn

Abstract: A trace ammonia (NH_3) detection system based on the near-infrared fiber-optic cantilever-enhanced photoacoustic spectroscopy (CEPAS) is proposed. A fiber-optic extrinsic Fabry-Perot interferometer (EFPI) based cantilever microphone has been designed to detect the photoacoustic pressure signal. The microphone has many advantages, such as small size and high sensitivity. A near-infrared tunable erbium-doped fiber laser (EDFL) amplified by an erbium-doped fiber amplifier (EDFA) is used as a photoacoustic excitation light source. To improve the sensitivity, the photoacoustic signal is enhanced by a photoacoustic cell with a resonant frequency of 1624 Hz. When the wavelength modulation spectroscopy (WMS) technique is applied, the weak photoacoustic signal is detected by the second-harmonic detection technique. Trace NH_3 measurement experiments demonstrate that the designed fiber-optic CEPAS system has a linear response to concentrations in the range of 0 ppm – 20 ppm at the wavelength of 1522.448 nm. Moreover, the detection limit is estimated to be 3.2 ppb for a lock-in integration time of 30 s.

Keywords: Trace gas detection; photoacoustic spectroscopy; cantilever microphone; fiber-optic Fabry-Perot interferometer; near-infrared laser

Citation: Min GUO, Ke CHEN, Zhenfeng GONG, and Qingxu YU, "Trace Ammonia Detection Based on Near-Infrared Fiber-Optic Cantilever-Enhanced Photoacoustic Spectroscopy," *Photonic Sensors*, 2019, 9(4): 293–301.

1. Introduction

Trace ammonia (NH_3) detection is important for environment monitoring and medical diagnosis [1–3]. Among the proposed trace gas detection methods, laser photoacoustic (PA) spectroscopy (PAS) shows many technical advantages, such as small sample volume, high detection sensitivity, and continuous measurement ability [4–6].

When the modulated excitation laser is tuned to one of the vibrational-rotational transitions of targeted gas molecules, a portion of the gas molecules move up to the excited state. By nonradiative relaxation, the excited molecules move down to the ground state. As a result, the gas in the PA cell expands periodically and generates sound pressure waves. The PA pressure wave can be detected by an acoustic sensor, such as an electronic microphone. Since the concentration of the target gas is proportional to the amplitude of the PA pressure wave, the target gas can be quantitatively detected [7]. Webber *et al.* reported a PAS based NH_3 gas detection system by interrogating a transition near 1532 nm with a 500 mW power from an erbium-doped fiber amplifier (EDFA) [8]. A detection limit of 9 ppb was achieved with an

Received: 29 October 2018 / Revised: 19 February 2019

DOI: 10.1007/s13320-019-0545-x
Article type: Regular

integration time of 10 s. If the microphone noise is higher than the acoustic noise caused by the environment, the sensitivity of the gas detection system based on PAS can be effectively improved by increasing the sensitivity of acoustic sensors. Therefore, various high-sensitivity acoustic sensors have been proposed in recent years, such as quartz tuning fork [9–11], fiber-optic acoustic sensor [12–15], and optical cantilever [16–18]. Wu *et al.* developed a quartz-enhanced PAS (QEPAS) based NH_3 gas detection system. A distributed feedback (DFB) diode laser boosted by an EDFA combined with a quartz tuning fork was used for trace NH_3 detection. Experiments showed that the detection limit could reach 52 ppb [18]. Ma *et al.* reported a sensitive QEPAS based NH_3 sensor [20]. The detection limit was achieved to be 418.4 ppb with an integration time of 1 s, and the corresponding normalized noise equivalent absorption coefficient (NNEA) was $3.83\times10^{-8}\,\mathrm{cm^{-1}\cdot W\cdot Hz^{-1/2}}$.

Since the working frequency of the non-resonant PAS is usually lower than 200 Hz, a large-size cantilever microphone with high sensitivity in the low-frequency range is much more suitable for a non-resonant PA cell. For the traditional cantilever-enhanced PAS (CEPAS), a Michelson interferometer is used to detect the dynamic displacement of the cantilever [21]. For low-frequency acoustic detection, a large-size cantilever has higher response. Therefore, when detecting trace gases, the CEPAS can be used to improve the sensitivity. However, the Michelson interferometer based optical cantilever sensor is difficult to be installed in the PA cell due to its large size and complex structure. Moreover, in the reported CEPAS systems, the cantilever and the PA cell both work in the non-resonant state. Therefore, the gas detection sensitivity is limited by the large $1/f$ noise with low working frequency.

In this paper, a fiber-optic CEPAS based trace NH_3 gas detection system is presented. A fiber-optic extrinsic Fabry-Perot (F-P) interferometer (EFPI) based cantilever microphone has been designed to detect the PA pressure signal. A near-infrared tunable erbium-doped fiber laser (EDFL) amplified by an EDFA is used as a PA excitation light source. To improve the sensitivity, the PA signal is enhanced by a resonant PA cell. The ability to detect ultra-low concentrations of NH_3 has been demonstrated at the wavelength of 1522.448 nm.

2. Principles

2.1 Principle of the EFPI based cantilever microphone

For an EFPI based cantilever microphone, the extrinsic F-P cavity is formed by the air gap between the free-vibration cantilever and the cleaved fiber endface. When the PA pressure is applied to the cantilever, the length of the F-P cavity will change periodically as the sound pressure changes. The EFPI can be regarded as a dual-beam interferometer. Therefore, when the intensity of incident light with a wavelength of λ is I_0, the reflected light intensity (I_r) can be expressed as [22, 23]

$$I_r = 2I_0\left[1+\gamma\cos\left(\frac{4\pi}{\lambda}\left(d_0+\Delta d\sin(\omega t)\right)+\pi\right)\right] \quad (1)$$

where γ is the fringe visibility of the interference fringe, d_0 is the length of the F-P cavity in a static state, Δd is the length variation of the F-P cavity, t is the time, and ω is the angle frequency of the sound wave.

To achieve the highest sensitivity and maximum linear operating range, the central wavelength of the probe laser should be kept at the quadrature point which lies at the maximum slope position of the interference fringe [24, 25]. With this demodulation method, the alternating-current (AC) component of the reflected light intensity can be described as follows:

$$I_r = 2I_0\gamma\frac{4\pi}{\lambda}\Delta d\sin(\omega t). \quad (2)$$

From (2), the variation of the F-P cavity length can be obtained by detecting the change in the

reflected light intensity, and then the PA signal can be demodulated.

2.2 Principle of the resonant PAS

Due to the superposition of longitudinal, azimuthal, and radial eigenmodes, several resonant acoustic modes can exist in the PA cavity [26]. If the modulation frequency of the light source coincides with one of the resonance frequencies of the PA tube, a standing acoustic wave is excited, and the PA tube works as an acoustic amplifier. Currently, the first-order longitudinal resonance PAS is one of the most commonly used high-sensitivity trace gas detection methods [27–30].

The combination of the wavelength modulation spectroscopy (WMS) and second-harmonic detection is the most effective way to eliminate the interference of wavelength-independent PA signals from the absorptions of the optical window and the cell wall [8, 31]. The generated wavelength-independent PA pressure may reach to mili-Pascal (mPa) level. Therefore, when the tunable laser is wavelength modulated, the influence of background noise on PA measurement can be almost completely eliminated by the second-harmonic detection technology.

3. Fiber-optic cantilever microphone manufacturing method and its characteristics

3.1 Manufacturing method of the cantilever microphone

Figure 1(a) shows the structure diagram of the sensor head. The cleaved endface of the fiber and the free-vibration cantilever together form an EFPI [29, 30, 32, 33]. The stainless steel shell is used to fix the ceramic ferrule and the cantilever diaphragm. Figure 1(b) shows the finite element analysis model. A rectangular stainless steel cantilever acts as an acoustically sensitive component. The analysis result shows that the width has little influence on the natural frequency of the cantilever. Meanwhile, when the cantilever thickness is 10 μm, the relationship between the natural frequency and cantilever length is analyzed by simulation, as shown in Fig. 2. In this paper, the cantilever with a length of 2.1 mm is selected. The analysis result shows that the natural frequency of the rectangular stainless steel cantilever is 1811 Hz. Figures 1(c) and 1(d) present the side view and front view of the cantilever microphone, respectively. A 1064 nm fiber laser marker (YLP-F10, Han's Laser) is used to manufacture the cantilever on a thin stainless steel diaphragm having a thickness of 10 μm. The dimension of the rectangular cantilever is 2.1 mm × 1 mm.

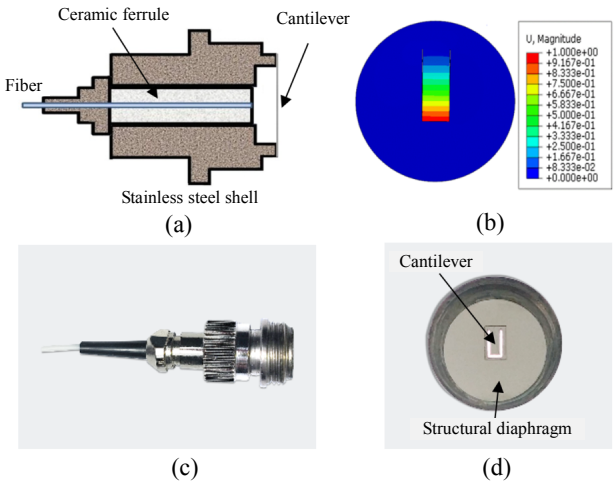

Fig. 1 Schematic diagram of the cantilever microphone: (a) structure diagram of the cantilever microphone, (b) finite element analysis model, (c) side view, and (d) front view of the cantilever microphone.

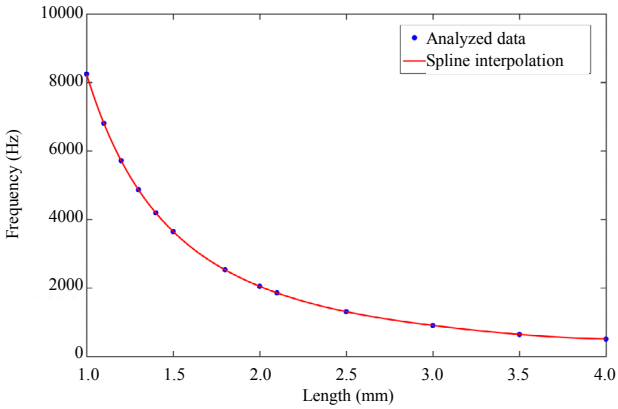

Fig. 2 Simulated relationship between the natural frequency and the length of a rectangular cantilever with a thickness of 10 μm.

3.2 Features of the cantilever microphone

The interference spectrum of the cantilever sensor is measured by a wavelength interrogator (si720, Micron Optics Inc.), as shown in Fig. 3. The F-P cavity length is demodulated to be 1305 μm using the fast Fourier transform (FFT) based demodulation method [34]. The PA pressure is demodulated by the interference-intensity demodulation mechanism [24, 25]. For the long cavity length sensor, environmental perturbations to the measurement can be eliminated by stabilizing the working point.

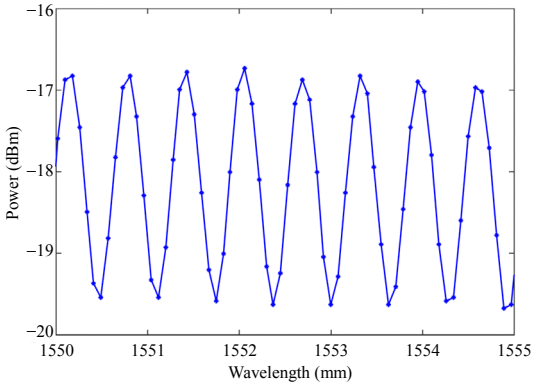

Fig. 3 Reflection interference spectrum of the manufactured cantilever sensor.

The designed cantilever microphone has been tested by an acoustic pressure test system [35]. In order to measure the sensitivity of the manufactured cantilever sensor, the acoustic pressure is adjusted to 10 mPa. Figure 4 shows the time domain response of the detected acoustic signal at the frequency of 1624 Hz. The acoustic pressure response of the designed cantilever microphone is measured in the range from 0 Pa to 0.2 Pa, as shown in Fig. 5. It indicates that when the acoustic pressure changes, the response changes accordingly. A linear fitting of the data points is applied. The fitting result shows that the regression line is very close to the actual data point. The calculated *R*-square value is equal to 0.9998, and the estimated acoustic pressure sensitivity is 1030 mV/Pa. Furthermore, the cantilever deflection can be calculated to be 2102 nm/Pa at 1624 Hz by using the method described in our previous work [32].

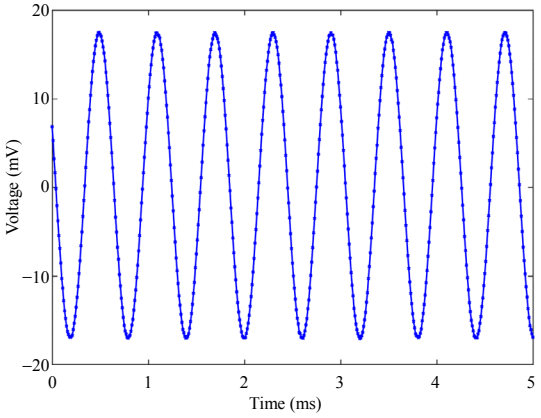

Fig. 4 Demodulated time-domain acoustic signal at 1624 Hz.

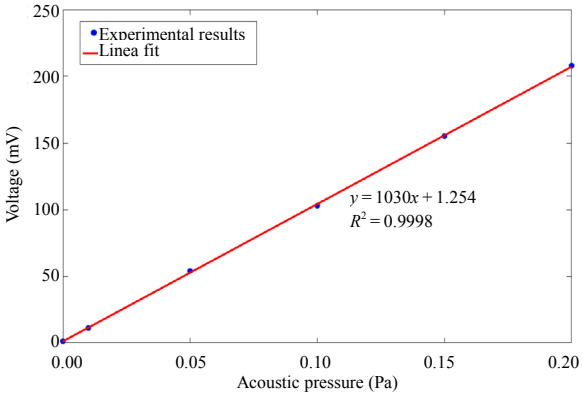

Fig. 5 Measured acoustic pressure response of the fiber-optic EFPI based cantilever microphone.

4. Photoacoustic experimental results and discussion

4.1 Photoacoustic experimental setup

Figure 6 shows the experimental setup for the fiber-optic CEPAS system. This system is comprised of four modules: a near-infrared tunable laser source, a PA cell, a PA signal detector, and a signal processor. A near-infrared tunable EDFL is designed as a PA excitation light source. Wavelength modulation of the EDFL is realized by using a tunable fiber-optic F-P filter (FFP-TF2, Micron Optics), whose free spectral range (FSR) is 100 nm. A combined signal of sawtooth and sine waves, which is supplied by a homemade lock-in amplifier (LIA), is used to drive the tunable F-P filter. The output light of the EDFL propagates to an EDFA. As a result, a PA excitation light source with an output power of 1000 mW is obtained. The excitation light

is then incident into the PA cell by a fiber collimator. An acoustic resonant tube and two buffer chambers together constitute the first-order longitudinal resonant PA cell. The acoustic resonance tube is a cylindrical brass tube with a diameter of 10 mm and a length of 100 mm. On the one hand, in order to reduce the NH_3 molecular adsorption and desorption effects on the surface of the tube wall, the temperature of the PA cell is maintained at 45 ℃. On the other hand, considering that the adsorption and desorption during gas transport can be greatly reduced by shortening the gas pipeline and increasing the flow rate, the length of the inlet pipeline is shortened to be ~50 cm, and the flow rate is set to be 2000 sccm. Moreover, the gas to be measured flows in the measurement system for 3 minutes before the measurement, so that the gas can be sufficiently balanced in the PA cell. As a result, the error of the prepared NH_3/N_2 gas concentration can be dramatically reduced. A gold-plated mirror is installed to reflect almost all of the laser back to increase the intensity of the PA signal. The air inlet and outlet, which are controlled by two valves, are located in two buffer chambers, respectively. The amplitude of the PA signal is the largest at the antinode, and the antinode is located in the middle of the resonant tube. Therefore, the microphone is installed in the middle of the resonator. The PA signal causes the vibration of the cantilever. As a result, the length of the F-P cavity changes periodically. The PA signal detection module, which mainly consists of a DFB laser, a fiber coupler, a fiber circulator and two photodiodes (PDs), converts the variation of the F-P cavity length to an alternate electrical signal by using the interference-intensity demodulation method. To keep track of the quadrature point, the wavelength of the DFB laser is tuned by controlling its injection current. However, the tuning range of the DFB laser is limited from 1550.2 nm to 1550.7 nm. If the operating point drifting out of the tuning range, the wavelength of the DFB laser can be recycled to continuously track the quadrature point [24]. Subsequently, the weak PA signal is extracted by the LIA. A control and signal processing program is developed by LabVIEW in a computer.

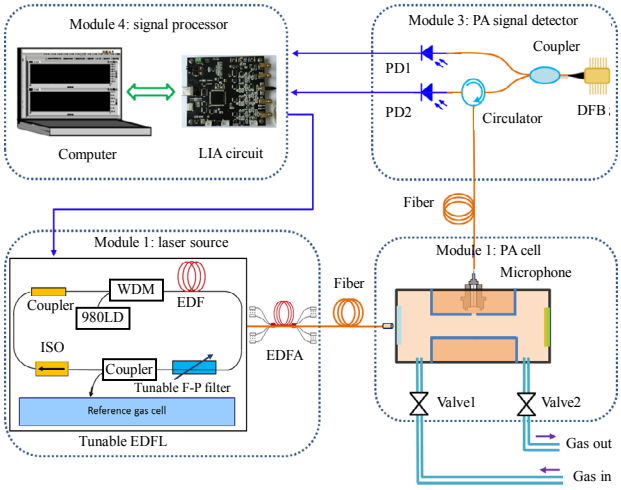

Fig. 6 Schematic diagram of the experimental setup.

4.2 Photoacoustic experimental results

To select the optimal operating frequency, the amplitude-frequency response of the PA system is measured from 1520 Hz to 1720 Hz by scanning the laser modulation frequency from 760 Hz to 860 Hz, when the PA cell is filled with a 20 ppm NH_3/N_2 gas mixture and the wavelength of the EDFL is maintained at 1522.448 nm. Figure 7 shows the amplitude-frequency response by using WMS and the second harmonic detection techniques. As shown, the resonant frequency is 1624 Hz. Since the natural frequency of the cantilever is about 1.8 kHz, the responsivities near 1.8 kHz are much higher. Therefore, the measured amplitude-frequency response curve is asymmetric.

Experiments with different concentrations of NH_3 measurements are carried out by the designed fiber-optic CEPAS system. Two mass flow controllers (MFCs) (D07-19, SevenStar Electronics), a bottle of high purity N_2 gas and a bottle of 20 ppm NH_3/N_2 gas are used for the preparation of experimental gases. A variety of gas concentrations are obtained by controlling the flow rate ratio of the

two MFCs. After filling the PA cell with the gas mixture, the valves are closed to isolate the environmental noise. In addition, the pressure in the PA cell is maintained at 1 atm during the PA measurement. The wavelength modulation frequency of the EDFL is 812 Hz, which is half the first-order resonant frequency of the PA cell. The wavelength of the EDFL is scanned from 1522.1 nm to 1522.7 nm with a scanning period of 30 s. The second-harmonic PA signals with different NH_3 concentrations are measured by using the WMS technique, as shown in Fig. 8.

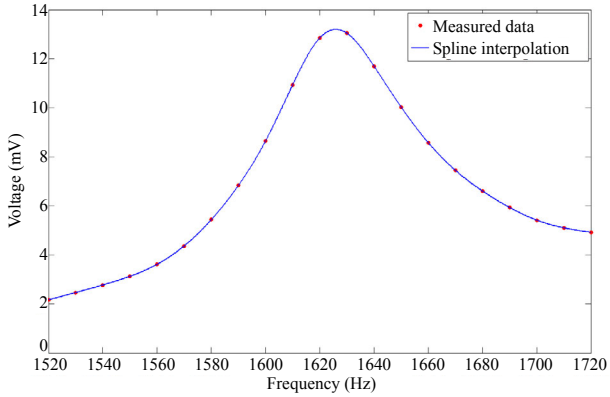

Fig. 7 Frequency response of the PAS system.

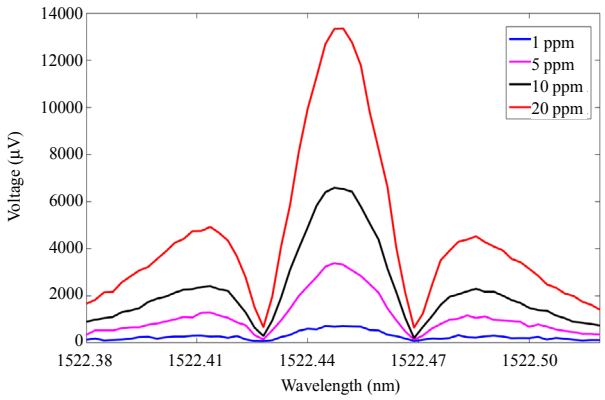

Fig. 8 Second harmonic signals of different concentrations of NH_3 with the laser modulation frequency of 812 Hz.

Gaussian fitting is used to search the peak value of the measured spectrum near the central wavelength of 1522.448 nm. Figure 9 shows the PA signals with different NH_3 concentrations. Each point represents the average value of the peaks of the second harmonic signal. The points corresponding to different concentrations of NH_3 have good linearity. The results of the linear fitting show that the *R*-square value is equal to 0.9997, and the fiber-optic CEPAS system has a response of 660.5 μV/ppm for trace NH_3 detection. By using the interference-intensity demodulation method, the PA demodulator works in the linear range when the vibration amplitude of the cantilever is less than 100 nm. According to Figs. 5 and 9, the PA pressure is less than 13.2 mPa, the maximum vibration amplitude can be estimated to be 27.7 nm with the responsivity of 2102 nm/Pa. Therefore, the PA demodulator works in the linear response range when the NH_3 concentration ranges from 0 ppm to 20 ppm.

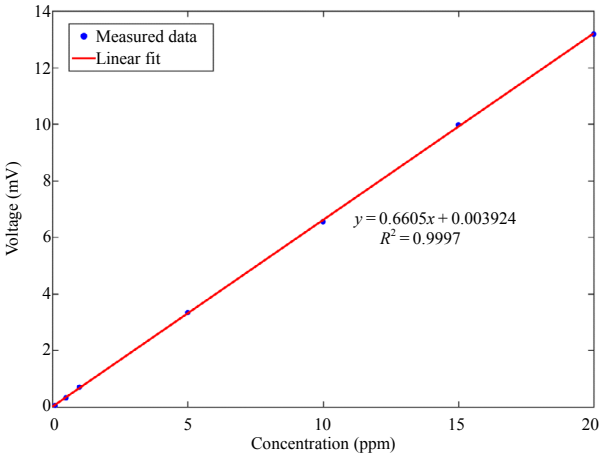

Fig. 9 Measured photoacoustic signals of different NH_3 concentrations.

To measure the background noise, high purity N_2 gas is filled into the PA cell, and the noise signal is recorded by the designed fiber-optic CEPAS system. Both EDFL and EDFA are in the working state during the experiment. The sawtooth signal becomes a fixed direct-current (DC) voltage, and the average wavelength of the laser is maintained at 1522.448 nm. The integration time of the lock-in amplifier is set to be 30 s. Figure 10 shows the recorded voltage of noise as a function of time. The calculation result of the voltage noise level (1σ) is 2.1 μV. Combined with the responsivity of 660.5 μV/ppm, the detection limit is estimated to be 3.2 ppb.

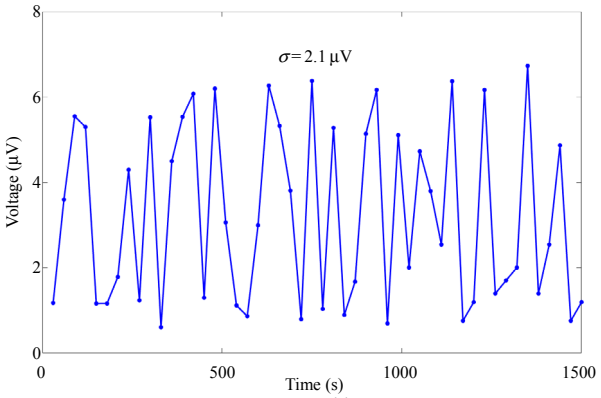

Fig. 10 Recorded voltage of noise as a function of time with the cell filled with pure N_2.

To further evaluate the performance of the fiber-optic CEPAS system, it is worth to calculate the *NNEA* coefficient, which normalizes the sensitivity performance of the gas detection system to the excitation power and absorption line strength [36, 37]. The *NNEA* coefficient can be expressed as

$$NNEA = \frac{\alpha_{\min} P}{\sqrt{ENBW}} \quad (3)$$

where $\alpha_{\min}$ is the minimum detectable absorption coefficient, P is the power of the laser light, and *ENBW* is the equivalent noise detection bandwidth of the signal detection system. For a 30 s lock-in integration time, the *ENBW* is equal to 0.00833 Hz. In addition, $\alpha_{\min}$ can be obtained to be 2.35×10^{-10} cm^{-1}, according to the detection limit of 3.2 ppb. As a result, the *NNEA* coefficient can be calculated to be $2.6\times10^{-9}\,cm^{-1}\cdot W\cdot Hz^{-1/2}$. In further research, in order to improve the detection sensitivity, the photoacoustic cell and cantilever with the similar resonance frequency will be selected, and the photoacoustic signal will be amplified by a dual resonance at this frequency. When the cantilever works in the resonant state, the Brown noise will increase greatly, and we will improve the signal-to-noise ratio by optimizing the operating parameters of the system [38].

5. Conclusions

In this paper, we present a fiber-optic CEPAS for trace NH_3 gas detection, which combines a fiber-optic EFPI based cantilever microphone and a first-order longitudinal resonant PA cell. A near-infrared EDFL combined with an EDFA is applied as the PA excitation light. The dimension and the thickness of the cantilever are 2.1 mm×1 mm and 10 μm, respectively. At the frequency of 1624 Hz, the sensitivity of the designed cantilever sensor is 1030 mV/Pa. With the methods of WMS and second-harmonic detection, different concentrations of trace NH_3 gas have been measured around the wavelength of 1522.448 nm. Experimental result shows that the designed fiber-optic CEPAS system has a linear response of 660.5 μV/ppm. Furthermore, the detection limit (1σ) is 3.2 ppb for an integration time of 30 s. In addition, the *NNEA* coefficient for NH_3 is calculated as $2.6\times10^{-9}\,cm^{-1}\cdot W\cdot Hz^{-1/2}$. In this system, the cantilever does not work in the resonant state. The PA signal can be further enhanced by the dual resonance of the cantilever and the PA cell. Moreover, in order to further reduce the adsorption of ammonia gas, the PA cell can be made of low surface energy materials, such as Teflon polytetrafluoroethylene.

Acknowledgment

This work is supported by the Fundamental Research Funds for the Central Universities [Grant No. DUT 18RC (4)040].

References

[1] X. F. Niu, Y. B. Zhong, R. Chen, F. Wang, and D. Luo, "Highly sensitive and selective liquid crystal optical sensor for detection of ammonia," *Optics Express*, 2017, 25(12): 13549–13556.

[2] M. J. Thorpe, B. C. David, M. S. Kirchner, and J. Ye, "Cavity-enhanced optical frequency comb spectroscopy: application to human breath analysis," *Optics Express*, 2008, 16(4): 2387–2397.
[3] M. Pisco, M. Consales, S. Campopiano, R. Viter, V. Smyntyna, M. Giordano, *et al.*, "A novel optochemical sensor based on SnO_2 sensitive thin film for ppm ammonia detection in liquid environment," *Journal of Lightwave Technology*, 2006, 24(12): 5000–5007.
[4] L. Dong, J. Wright, B. Peters, B. A. Ferguson, F. K. Tittel, and S. M. Whorter, "Compact QEPAS sensor for trace methane and ammonia detection in impure hydrogen," *Applied Physics B*, 2012, 107(2): 459–467.
[5] Q. Wang, Z. Wang, and W. Ren, "Theoretical and experimental investigation of fiber-ring laser intracavity photoacoustic spectroscopy (FLI-PAS) for acetylene detection," *Journal of Lightwave Technology*, 2006, 35(20): 4519–4525.
[6] J. W. Wang, W. Zhang, L. Li, and Q. Yu, "Breath ammonia detection based on tunable fiber laser photoacoustic spectroscopy," *Applied Physics B*, 2011, 103(2): 263–269.
[7] K. Chen, Z. F. Gong, and Q. X. Yu, "Fiber-amplifier-enhanced resonant photoacoustic sensor for sub-ppb level acetylene detection," *Sensors and Actuators A: Physical*, 2018, 274: 184–188.
[8] M. E. Webber, M. Pushkarsky, and C. K. Patel, "Fiber-amplifier-enhanced photoacoustic spectroscopy with near-infrared tunable diode lasers," *Applied Optics*, 2003, 42(12): 2119–2126.
[9] A. A. Kosterev, Y. A. Bakhirkin, R. F. Curl, and F. Tittel, "Quartz-enhanced photoacoustic spectroscopy," *Optics Letters*, 2002, 27(21): 1902–1904.
[10] L. K. Guo, X. Y. Guo, H. M. Yi, W. D. Chen, W. J. Zhang, and X. M. Gao, "Off-beam quartz-enhanced photoacoustic spectroscopy," *Optics Letters*, 2009, 34(10): 1594–1596.
[11] S. Borri, P. Patimisco, I. Galli, D. Mazzotti, G. Giusfredi, N. Akikusa, *et al.*, "Intracavity quartz-enhanced photoacoustic sensor," *Applied Physics Letters*, 2014, 104(9): 091114-1–091114-4.
[12] Y. C. Cao, W. Jin, H. L. Ho, and J. Ma, "Miniature fiber-tip photoacoustic spectrometer for trace gas detection," *Optics Letters*, 2013, 38(4): 434–436.
[13] X. F. Mao, X. L. Zhou, Z. F. Gong, and Q. X. Yu, "An all-optical photoacoustic spectrometer for multi-gas analysis," *Sensors and Actuators B: Chemical*, 2016, 232: 251–256.
[14] Y. Z. Tan, C. Z. Zhang, W. Jin, F. Yang, H. L. Ho, and J. Ma, "Optical fiber photoacoustic gas sensor with graphene nano-mechanical resonator as the acoustic detector," *IEEE Journal of Selected Topics in Quantum Electronics*, 2017, 23(2): 199–209.
[15] Z. F. Gong, K. Chen, Y. Yang, X. L. Zhou, W. Peng, and Q. X. Yu, "High-sensitivity fiber-optic acoustic sensor for photoacoustic spectroscopy based traces gas detection," *Sensors and Actuators B: Chemical*, 2017, 247: 290–295.
[16] V. Koskinen, J. Fonsen, K. Roth, and J. Kauppinen, "Progress in cantilever enhanced photoacoustic spectroscopy," *Vibrational Spectroscopy*, 2008, 48(1): 16–21.
[17] J. Peltola, T. Hieta, and M. Vainio, "Parts-per-trillion-level detection of nitrogen dioxide by cantilever-enhanced photo-acoustic spectroscopy," *Optics Letters*, 2015, 40(13): 2933–2936.
[18] H. Moser and B. Lendl, "Cantilever-enhanced photoacoustic detection of hydrogen sulfide (H_2S) using NIR telecom laser sources near 1.6 μm," *Applied Physics B*, 2016, 122(4): 83-1–83-11.
[19] H. P. Wu, L. Dong, X. L. Liu, H. D. Zheng, X. K. Yin, W. G. Ma, *et al.*, "Fiber-amplifier-enhanced QEPAS sensor for simultaneous trace gas detection of NH_3 and H_2S," *Sensors*, 2015, 15(10): 26743–26755.
[20] Y. F. Ma, Y. He, Y. Tong, X. Yu, and F. K. Tittel, "Ppb-level detection of ammonia based on QEPAS using a power amplified laser and a low resonance frequency quartz tuning fork," *Optics Express*, 2017, 25(23): 29356–29364.
[21] J. Kauppinen, K. Wilcken, I. Kauppinen, and V. Koskinen, "High sensitivity in gas analysis with photoacoustic detection," *Microchemical Journal*, 2004, 76(1): 151–159.
[22] Q. X. Yu and X. L. Zhou, "Pressure sensor based on the fiber-optic extrinsic Fabry-Perot interferometer," *Photonic Sensors*, 2011, 1(1): 72–83.
[23] K. Chen, X. L. Zhou, B. K. Yang, W. Peng, and Q. X. Yu, "A hybrid fiber-optic sensing system for down-hole pressure and distributed temperature measurements," *Optics & Laser Technology*, 2015, 35: 82–87.
[24] X. F. Mao, X. L. Zhou, and Q. X. Yu, "Stabilizing operation point technique based on the tunable distributed feedback laser for interferometric sensors," *Optics Communications*, 2016, 361: 17–20.
[25] X. F. Mao, S. Z. Yuan, P. C. Zheng, and P. C. Zheng, "Stabilized fiber-optic Fabry–Perot acoustic sensor based on improved wavelength tuning technique," *Journal of Lightwave Technology*, 2017, 73(11): 2311–2314.
[26] M. Hippler, C. Mohr, K. A. Keen, and E. D. M. Naghten, "Cavity-enhanced resonant photoacoustic spectroscopy with optical feedback cw diode lasers: a novel technique for ultratrace gas analysis and high-resolution spectroscopy," *The Journal of Chemical Physics*, 2010, 133(4): 289–297.
[27] A. Boschetti, D. Bassi, E. Iacob, and S. Iannaotta, "Resonant photoacoustic simultaneous detection of methane and ethylene by means. of a 1.63-μm diode laser," *Applied Physics B*, 2002, 74(3): 273–278.

[28] J. W. Wang, W. Zhang, L. R. Liang, and Q. X. Yu, "Tunable fiber laser based photoacoustic spectrometer for multi-gas analysis," *Sensors and Actuators B: Chemical*, 2011, 160(1): 1268–1272.

[29] K. Chen, Q. X. Yu, Z. F. Gong, M. Guo, and C. Qu, "Ultra-high sensitive fiber-optic Fabry-Perot cantilever enhanced resonant photoacoustic spectroscopy," *Sensors and Actuators B: Chemical*, 2018, 268: 205–209.

[30] K. Chen, Z. H. Yu, Z. F. Gong, and Q. X. Yu, "Lock-in white-light-interferometry-based all-optical photoacoustic spectrometer," *Optics Letters*, 2018, 43(20): 5038–5041.

[31] D. Viveiros, J. Ferreira, S. O. Silva, J. Ribero, D. Flores, J. L. Santos, *et al.*, "Ammonia sensing system based on wavelength modulation spectroscopy," *Photonic Sensors*, 2015, 5(2): 109–115.

[32] K. Chen, Z. F. Gong, M. Guo, S. C. Yu, C. Qu, X. L. Zhou, *et al.*, "Fiber-optic Fabry-Perot interferometer based high sensitive cantilever microphone," *Sensors and Actuators A: Physical*, 2018, 279: 107–112.

[33] K. Chen, Z. H. Yu, Q. X. Yu, M. Guo, Z. H. Zhao, C. Qu, *et al.*, "Fast demodulated white-light interferometry-based fiber-optic Fabry–Perot cantilever microphone," *Optics Letters*, 2018, 43(14): 3417–3420.

[34] Z. H. Yu and A. B. Wang, "Fast white light interferometry demodulation algorithm for low-finesse Fabry-Pérot sensors," *IEEE Photonics Technology Letters*, 2015, 27(8): 817–820.

[35] Z. F. Gong, K. Chen, X. L. Zhou, Y. Yang, Z. H. Zhao, H. L. Zou, *et al.*, "High-sensitivity Fabry-Perot interferometric acoustic sensor for low-frequency acoustic pressure detections," *Journal of Lightwave Technology*, 2017, 35(24): 5276–5279.

[36] S. Zhou, M. Slaman, and D. Iannuzzi, "Demonstration of a highly sensitive photoacoustic spectrometer based on a miniaturized all-optical detecting sensor," *Optics Express*, 2017, 25(15): 17541–17548.

[37]H. P. Wu, L. Dong, H. D. Zheng, Y. J. Yu, W. G. Ma, L. Zhang, *et al.*, "Beat frequency quartz-enhanced photoacoustic spectroscopy for fast and calibration-free continuous trace-gas monitoring," *Nature Communications*, 2017, 8: 15331-1–15331-8.

[38] B. D. Adamson, J. E. Sader, and E. J. Bieske, "Photoacoustic detection of gases using microcantilevers," *Journal of Applied Physics*, 2009, 106: 114510-1–114510-4.